Volume 53
Number 39
21 October 2024
Pages 16079-16424

Dalton Transactions

An international journal of inorganic chemistry

rsc.li/dalton

ISSN 1477-9226

ROYAL SOCIETY OF CHEMISTRY

PAPER

Dmitri Gelman, Evamarie Hey-Hawkins *et al.*
Synthesis and catalytic activity of heterobimetallic Au/M (M = Rh^{III}, Ir^{III}) complexes with ditopic mono- and triphosphane ligands

Dalton Transactions

ROYAL SOCIETY OF CHEMISTRY

PAPER

View Article Online
View Journal | View Issue

Cite this: *Dalton Trans.*, 2024, **53**, 16159

Synthesis and catalytic activity of heterobimetallic Au/M (M = Rh^{III}, Ir^{III}) complexes with ditopic mono- and triphosphane ligands†

Ivana Predarska, [a] Wieland Körber,[a] Peter Lönnecke, [a] Dmitri Gelman [*b] and Evamarie Hey-Hawkins [*a]

Received 28th April 2024,
Accepted 23rd June 2024

DOI: 10.1039/d4dt01247j

rsc.li/dalton

A series of heterobimetallic complexes Au/M (M = Rh^{III}, Ir^{III}) were prepared on the basis of two ditopic ligands: a monophosphane ligand **L1**H and a triphosphane ligand **L2**H. The complexes were fully characterised, including single-crystal X-ray diffraction studies. Catalytic activity of cationic **L1**/Au^{I}/Ir^{III} and **L2**/Au^{I}/Ir^{III} bis(trifluoromethane)sulfonimide was analysed through their capacity to induce allenyl ether rearrangement and cycloisomerisation of *N*-propargyl benzamide. While cationic **L1**/Au^{I}/Ir^{III} showed some ability to induce allenyl ether rearrangement, no conversion was observed for cationic **L2**/Au^{I}/Ir^{III}. Similarly, *N*-propargyl benzamide could undergo cycloisomerisation in the presence of cationic **L1**/Au^{I}/Ir^{III}, whereas cationic **L2**/Au^{I}/Ir^{III} was again inactive. These findings highlight how crucial the surroundings of the metal centre are to the catalytic activity. Catalytic activity is only possible when Au has a free coordination site; the gold complex becomes inactive when the tridentate ligand is present.

Introduction

In the context of homogeneous catalysis using organometallic compounds, the focus has historically been on single-site catalysts to prevent the formation of multinuclear compounds.[1] However, in biological systems, especially those involved in redox transformations of small molecules like water or carbon dioxide, multimetallic assemblies and their reactivity are crucial.[2] Some biological systems rely on the synergistic activation of substrates by multiple metal centres.[3] For instance, nickel-containing carbon monoxide dehydrogenase (Ni–CODH) utilises both nickel and iron centres to convert carbon dioxide to carbon monoxide and *vice versa*.[4,5]

Comprehension of the interactions and catalytic characteristics of bi- and polymetallic centres within metalloenzymes has exerted a substantial influence on various scientific disciplines, including the realm of synthetic chemistry. Significant attention has been garnered in the field of coordination chemistry and catalysis, particularly regarding multimetallic complexes.[2] These complexes offer a unique platform for expanding the repertoire of homogeneous catalysts. Heterobimetallic compounds, composed of two different metal ions incorporated into a singular ligand framework, have the potential to broaden the range of redox states and coordination possibilities for substrates due to intermetallic collaboration driven by electronic interactions or the concurrent activation of one or more substrates.[6–8] The versatile nature of metal pairings in heterobimetallic complexes offers a possibility to streamline diverse catalytic processes into a unified one-pot tandem reaction.[7–10] As a result, these complexes have been documented to exhibit superior catalytic activity and selectivity compared to their mono- and homobimetallic counterparts.[9,10]

Despite their distinctive catalytic characteristics, the synthesis of well-defined heterobimetallic complexes and their practical application in catalysis presents many challenges on account of the potential for non-specific chelation of metal ions by both binding sites or ion exchange in solution. To mitigate this, the construction of elaborate ligand scaffolds characterised by two distinct binding domains, with the capacity to discriminate between two distinct metal ions, is indispensable.[11]

One class of ligands that has received steadily growing interest in the context of homogeneous catalysis over the past decades is pincer ligands and their associated metal complexes.[12,13] That is due to their robust tridentate coordination, effective metal–ligand cooperation, and high thermal and kinetic stability, thereby minimising metal leaching

[a]*Leipzig University, Faculty of Chemistry and Mineralogy, Institute of Inorganic Chemistry, Johannisallee 29, 04103 Leipzig, Germany. E-mail: hey@uni-leipzig.de*
[b]*The Hebrew University, Institute of Chemistry, Edmond Safra Campus, 9190401 Jerusalem, Israel. E-mail: dmitri.gelman@mail.huji.ac.il*

†Electronic supplementary information (ESI) available: NMR and mass spectra of **L1**H, **1–3**, **5–10**, and crystallographic data of **L1**H, **1–3**, **5**, **6**, **8–10**. CCDC 2322723–2322731. For ESI and crystallographic data in CIF or other electronic format see DOI: https://doi.org/10.1039/d4dt01247j

during the catalytic cycle. Additionally, fine-tuning of the electronic and steric properties of the metal centre can be afforded with these ligands.[14–17] A plethora of different types of pincer ligands have been developed over the years. Their complexes have been used as sensors, crystalline switches, and, most frequently, as precatalysts for various reactions.[14] Particularly relevant in catalysis are those containing phosphorus coordination sites owing to their ability to stabilise metal centres in high and low oxidation states.[18,19]

We have recently created a range of heterobimetallic complexes using a ditopic ligand setup (**L2**, Scheme 1) with a pincer PPP-type binding site and a phenylpyridine binding site. These include a Mo^0/Rh^{III}, Mo^0/Ir^{III}, Cr^0/Ir^{III}, W^0/Ir^{III} and a Co^0/Ir^{III} complex.[20–22] Among the described compounds, the Mo^0/Ir^{III} complex exhibited the highest activity in the context of homogeneous carbon dioxide hydrogenation, resulting in the formation of formate salts.[20,22] Herein, we are expanding this approach by introducing additional heterobimetallic Au/M complexes (M = Rh^{III}, Ir^{III}) built upon the same ligand system. Additionally, an analogous ligand with a monophosphane binding site was prepared (**L1**H, Scheme 1) and is hereby reported along with its corresponding Au/M complexes (M = Rh^{III}, Ir^{III}). Selected analogous complexes based on both ligands **L1**H and **L2**H were tested for their catalytic activity, namely, their capacity to induce allenyl ether rearrangement and cycloisomerisation of *N*-propagyl benzamide.

Results and discussion

Synthesis and characterisation of ligand L1H

The heteroditopic ligand **L1**H was designed to afford two distinct coordination sites.[24] The lithiation of 2-(4-bromophenyl) pyridine at −60 °C with ^{n}BuLi followed by the reaction with diisopropylchlorophosphane gave the monophosphane, which was protected *in situ* with sulfur, to yield **L1**H in 88% yield. Protection was required to avoid the coordination of phosphorus during the cyclometallation step. **L1**H was characterised by multinuclear NMR spectroscopy. Expectedly, for sulfurised tertiary phosphanes, the $^{31}P\{^1H\}$ NMR spectrum of **L1**H revealed a singlet at 66.4 ppm. The structure was further verified *via* high-resolution ESI(+) mass spectrometry and single crystal X-ray diffraction.

Cyclometallation

The cyclometallation step was performed according to the literature procedure.[23] The phosphane sulfide **L1**H was reacted with dimeric $[MCp^*Cl_2]_2$ (M = Rh, Ir) in the presence of excess NaOAc. The cyclorhodate complex **1** and cycloiridate complex **2** were isolated in 97% yield and fully characterised. In the $^{31}P\{^1H\}$ NMR spectra, singlets were observed at 67.0 ppm or 66.7 ppm for **1** or **2**, respectively. In the ^1H and $^{13}C\{^1H\}$ NMR spectra, cyclometallation leads to separate signals for each atom at the phenyl ring. Similarly, the methine protons are no longer equivalent in both complexes and split up into two sets of signals. Similar chemical shifts were found for most protons in the ^1H NMR spectra of both complexes. The only exception are the methyl protons of the Cp* moiety with a singlet signal at 1.70 ppm for **2** and 1.66 ppm for **1**. The $^{13}C\{^1H\}$ NMR spectra also show significant similarities, the difference being in the metal-bound carbon atoms: the cyclopentadienyl carbon atoms are observed at 96.3 ppm for **1**, split into a doublet due to the coupling with Rh ($^1J_{CRh}$ = 6.3 Hz). In comparison, a singlet at 89.1 ppm is observed for **2**. The phenyl ring carbon atoms resonate at 163.0 ppm (d, $^3J_{CP}$ = 8.8 Hz) for **2** and a doublet of doublets at 178.1 ppm (dd, $^1J_{CRh}$ = 32.5, $^3J_{CP}$ = 8.4 Hz) is observed for **1**. The comparable 2-phenylpyridine rhodium complex [RhCp*(ppy)Cl] showed a higher $^1J_{CRh}$ coupling constant of 86.8 Hz.[30] A similar drop in the $^1J_{CRh}$ coupling constant was observed for the rhodacycle of 2-(4-fluorophenyl)pyridine (dd, $^1J_{CRh}$ = 33.4, $^3J_{CF}$ = 4.3 Hz).[31]

Slow decomposition of the complexes was observed over time in $CDCl_3$ (followed by ^1H NMR spectroscopy). Single crystals suitable for X-ray diffraction analysis could be obtained by slow cooling of saturated solutions in MeOH (for **1**) or acetonitrile (ACN) (for **2**). The molecular structures are depicted in Fig. 1.

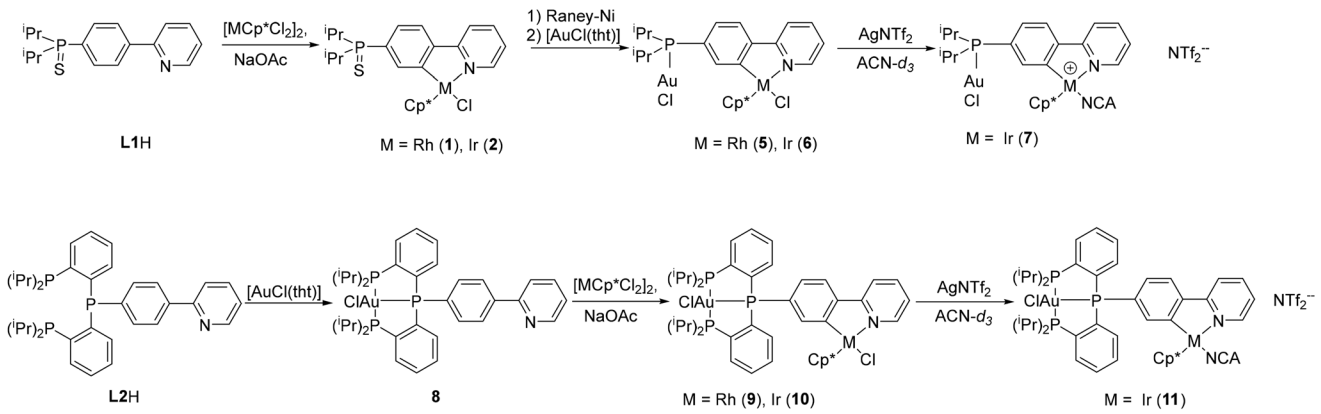

Scheme 1 Synthesis of heterometallic Au/M complexes (M = Rh, Ir; Cp* = C_5Me_5). **L2**H was described previously.[20]

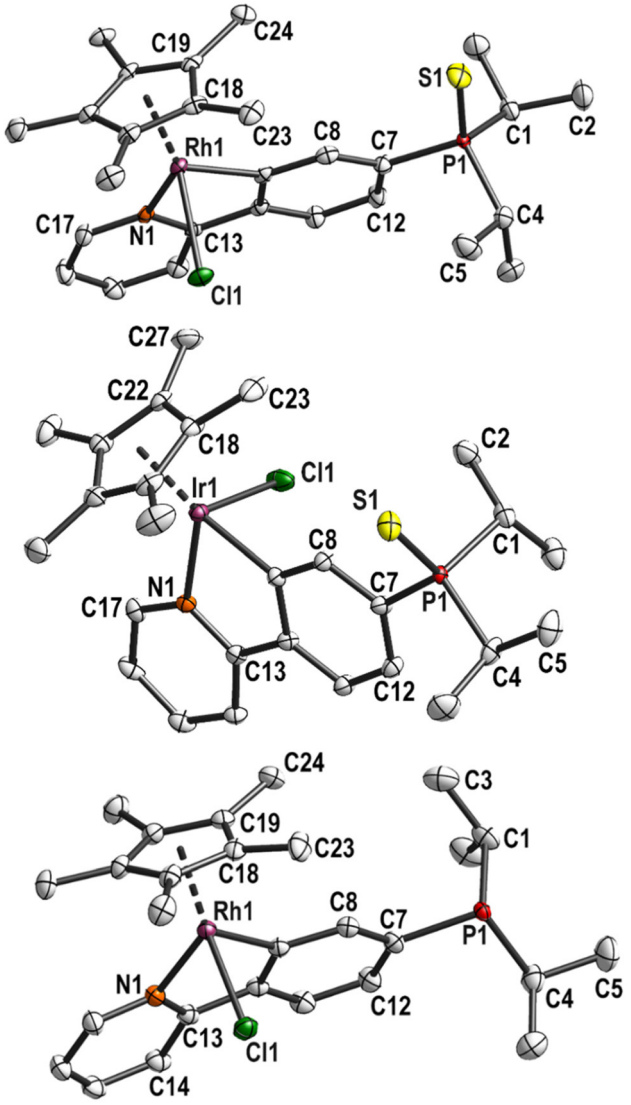

Fig. 1 Molecular structure and labelling scheme of complexes **1** (top), **2** (centre) and **3** (bottom). Hydrogen atoms are omitted for clarity and displacement ellipsoids are drawn at 50% probability level.

Complex **1** crystallised in the monoclinic space group $P2_1$ with one molecule and one cocrystallised methanol molecule in the asymmetric unit. The chloride ligand forms a hydrogen bond with the hydroxy group (d(O1–Cl1) = 3.220(4) Å). Compound **2** crystallised in the orthorhombic space group $Pna2_1$ with one molecule in the asymmetric unit. Both structures show a piano stool coordination of the metal centre. The bond lengths and angles are very similar to the closely related 2-phenylpyridine complexes previously published (see Table S2, ESI†).[30]

Compared to the parent complexes, the M1–C9 bond (2.036(1) Å for **1** and 2.032(5) Å for **2**) are shorter by 1–2 pm. Such subtle changes have been observed for complexes bearing other electron-withdrawing groups in *para* position (such as CN, CF_3, F) and show the higher acidity of the *ortho*-H compared to 2-phenylpyridine.[23,31–33] The M1–Cl1 bond is almost perpendicular to the C9–M1–N1 plane.

Desulfurisation

Several deprotection methods are known for phosphine sulfides.[34–36] Reduction of phosphine sulfides in complexes **1** and **2** with strong hydrides was avoided because of possible decomposition of the metallacycle, which was shown by Norton *et al.*[37] Addition of a strong nucleophilic phosphane, such as PEt_3 to the cyclorhodate complex **1**, did not result in the sulfur transfer, but over time led to complexation of Rh^{III}. Using freshly activated RANEY® nickel (RANEY®-Ni) in THF at 50 °C gave the phosphane **3**. The progress of the reaction was monitored by $^{31}P\{^1H\}$ NMR spectroscopy, and, if necessary, small amounts of activated RANEY®-Ni were added until conversion was completed. Due to the poor solubility of **1** and **2** in THF, the measurement time had to be increased to ensure all of the starting material was completely consumed. The free phosphane was directly used for further reactions after a rough yield determination to avoid side reactions, including oxidation or complexation.

Complex **3** was isolated and characterised by NMR spectroscopy, HR-ESI(+)-MS as well as single crystal X-ray diffraction, while complex **4** was not isolated, but used directly for the formation of heterometallic complex **6**. The $^{31}P\{^1H\}$ NMR spectra of both complexes display a singlet between 10 to 15 ppm depending on the solvent used and the coordinated metal. Compared to the sulfurised precursor, the ^1H NMR signals in **3** are shifted highfield in good accordance with the lesser electron-withdrawing effect of the free phosphane. The most affected protons are those of the phenylene and isopropyl groups. The same effect was observed in the $^{13}C\{^1H\}$ NMR spectrum for the phenyl carbon atom bound to phosphorus (shifted from 146.5 to 144.2 ppm).

Under high-resolution ESI(+)-MS conditions, the main signal at 508.1646 m/z could be attributed to the desired complex **3** with a lost chloride ligand $[M - Cl]^+$, typical for halide complexes.

Crystals of **3** (Fig. 1, bottom) were obtained by layering a THF solution with *n*-hexane. **3** crystallised in the monoclinic space group $P2_1n$ with one molecule in the asymmetric unit. Desulfurisation had little impact on the Rh–C9 bond length. The Rh–Cl1 bond is 1 pm shorter, possibly due to the lack of the hydrogen bond of the solvent observed in **1**. As in **1**, the Rh1–Cl1 bond is perpendicular to the N1–Rh–C1 plane. The sum of bond angles in the rhodacycle did not change (539.7° for **3**, 539.9° for **1** (ideal 540°)).

Gold complexation

The cyclometalated phosphane complexes **3** and **4** were reacted with [AuCl(tht)] (tht = tetrahydrothiophene) to give the heterobimetallic complexes **5** (M = Rh) and **6** (M = Ir) quantitatively (Scheme 1). It is worth noting that our attempt to reverse the order of metalation reactions were proved inefficient in the past.[20] The $^{31}P\{^1H\}$ NMR spectra of the reaction solutions indicated complete conversion by a downfield shift

of the signal to 60.0 ppm (from 10 to 15 ppm in **3** and **4**). The ^{1}H and $^{13}C\{^{1}H\}$ NMR spectra show similar features as observed for the sulfurised precursors. In $CDCl_3$, the ^{1}H NMR spectra showed very similar shifts for most signals, with the only exception of the methyl protons of the Cp* moiety with a singlet at 1.56 ppm for **5** and 1.71 ppm for **6**. For **5**, the signals in the aromatic region between 7.81 and 7.64 ppm (dt and dd) are well separated, but overlap to a multiplet for **6**. The $^{13}C\{^{1}H\}$ NMR spectra also show great similarities, the difference being in the metal-bound carbon atoms. The cyclopentadienyl carbon atoms are observed at 96.7 (d, $^{1}J_{CRh}$ = 6.3 Hz) for **5** and 89.0 ppm (s) for **6**. The phenyl ring carbon atoms are observed as a doublet of doublets at 179.8 ppm (dd, $^{1}J_{CRh}$ = 33.0, $^{3}J_{CP}$ = 9.1 Hz) for **5**, and as a doublet at 164.0 ppm (d, $^{3}J_{CP}$ = 9.7 Hz) for **6**.

Single crystals suitable for X-ray diffraction analysis of the heteronuclear complexes were obtained from a boiling saturated acetonitrile solution by stepwise cooling with a thermostat over several days. The use of a thermostat prevented the formation of powders. Attempts to crystallise **5** from a DCM solution with Et_2O or MeOH lead to decomposition. The compounds are more stable in chlorinated solvents, but solvent removal was accompanied by partial decomposition. On the other hand, the compounds were found to be stable toward light and in an acetonitrile solution.

Both complexes crystallised isostructurally in the monoclinic space group $P2_1$ with one molecule in the asymmetric unit. The Au1–P1 bond lengths of 2.245(1) Å (**5**) and 2.239(2) Å (**6**) as well as the Au1–Cl1 bond lengths (2.301(2) Å (**5**); 2.300(2) Å (**6**)) are comparable to other phosphane gold(I) complexes such as [AuCl(PPh_3)],[38] [AuCl(PCy_3)],[39] [AuCl(P^iPr_3)][40] and [AuCl(PCy_2Ph)].[41] The gold atoms are in linear coordination with P1–Au1–Cl1 bond angles of 176.75° (**5**) and 176.7° (**6**) (Fig. 2).

The bond lengths and angles around Rh and Ir are very similar to the precursor complexes, respectively. As there are no major deviations from the normal coordination environment, it can be assumed that both metal centres can work in tandem in catalysis. The P–Au–Cl unit in both complexes is oriented in the direction of the Cp* ligand with torsion angles Cp*(centroid)–M1···P1–Au1 around 15° (Table S3†). This is similar to the phosphane sulfide precursors and is probably the result of steric interaction between the isopropyl groups and the Cp* ligand. In the free phosphane rhodacycle complex **6**, this torsion angle amounts to 60°, which minimises the steric interaction of the isopropyl groups with the aryl group. Since there are greater steric interactions in the gold(I) complexes, the P atom is slightly dislocated from the phenyl plane by 0.271(7) Å (**5**) and 0.291(9) Å (**6**), respectively.

The intramolecular distances between the metal atoms are 6.2471(6) Å (**5**) and 6.2344(4) Å (**6**). The chloride ligands are further apart (8.025(3) Å (**5**) and 8.047(3) Å (**6**)) since the metal–chloride vectors are staggered (Cl1–Au1···M1–Cl2 torsion angles of 110.34(6)° (**5**) and 111.32(6)° (**6**)). The most similar dinuclear Au^{I}/Ir^{III} or Au^{I}/Rh^{III} complexes in the literature were bis-carbene complexes by Hahn *et al.* and showed a larger distance between the metal atoms in the solid state (Table S4†).[42]

Anion exchange reactions

Cationic piano-stool type complexes were found to work better for most catalytic reactions in comparison to their neutral counterparts,[43] due to the higher availability of the catalytically active species with a free active site for the reaction. Here, the ion exchange reaction of **6** was conducted by the addition of $AgNTf_2$ and subsequent isolation by the precipitated AgCl salt *via* filtration, as this might have an impact on the catalytic performance.[44]

The reaction was performed in CD_3CN which acts as a weak ligand and can prevent rapid exchange reactions. Due to the poor solubility of **6** in acetonitrile, CD_2Cl_2 was added. With one equiv. $AgNTf_2$, the reaction was incomplete, while two equiv. $AgNTf_2$ led to the formation of the desired bis-cationic complex **7**, which was investigated *in situ* by NMR spectroscopy and HRMS. No crystals could be obtained, and the stability upon solidification was questionable. HR-ESI(+)-MS showed the same signal as found for **6**, suggesting the presence of **6** ($[M - Cl]^+$) or the monocationic complex with one NTf_2 anion

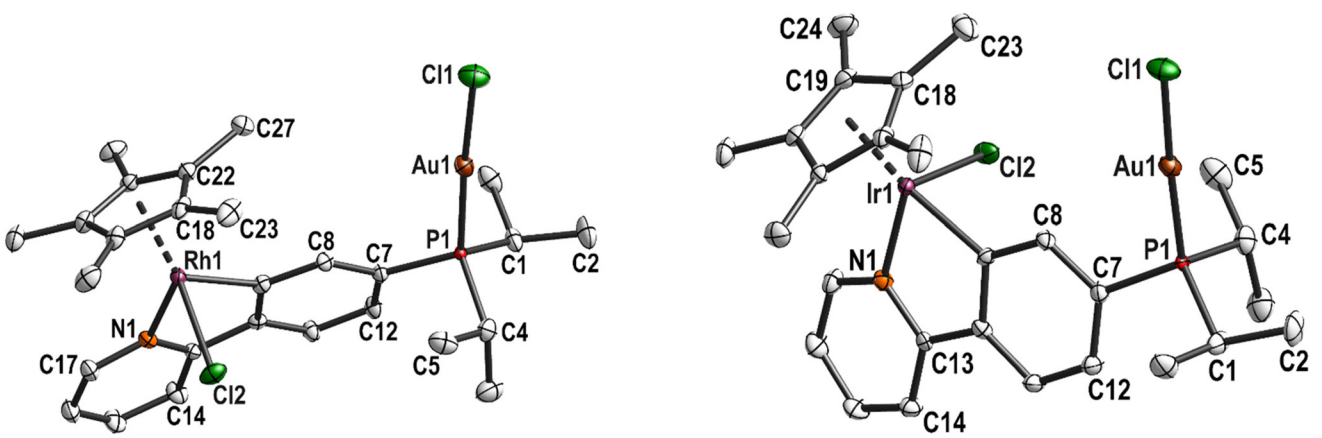

Fig. 2 Molecular structure and labelling scheme of complexes **5** (left) and **6** (right). Hydrogen atoms are omitted for clarity and displacement ellipsoids are drawn at the 50% probability level.

($[M - NTf_2]^+$) as an impurity. However, several other signals support the formation of the desired product, namely a signal corresponding to $[M - NTf_2]^+$ (m/z = 1075.1053, 37% rel. abundance), furthermore the acetonitrile adduct $[M - (NTf_2)_2 + (NCCH_3)_2]^{2+}$ (m/z = 438.6191, 1% rel. abundance), as well as the "naked" dinuclear complex $[M - (NTf_2)_2]^{2+}$ (m/z = 397.5958, <1% rel. abundance).

Synthesis and characterisation of complexes based on ligand L2H

The synthesis of the triphosphane ligand **L2**H was previously described by our group.[20] To afford heterobimetallic complexes based on this ditopic ligand, the two distinctively different coordination environments available were approached with stepwise coordination of the two metals.

Contrary to the monophosphane ligand **L1**H, in the case of **L2**H, at first, the phosphane site was employed in complexation using chlorido(tetrahydrothiophene)gold(I) ([AuCl(tht)]) as the gold(I) source. Complex **8** was obtained quantitatively and fully characterised with multinuclear NMR spectroscopy, ESI-MS, elemental analysis, and FT-IR. Compared to the complexes based on the monophosphane ligand **L1**H, the biggest difference is observed in the ^{31}P NMR spectrum with doublet and triplet signals displayed with a P,P coupling constant of *ca.* 115 Hz. Complex **8** showed high stability in DCM over weeks and did not manifest sensitivity toward light.

Crystals were obtained by layering a DCM solution of **8** with *n*-hexane. **8** crystallised in the monoclinic space group $P2_1/c$ with two independent molecules in the asymmetric unit (Fig. 3). The complex molecules are most likely marginally disordered with a ratio of 0.9845(4) : 0.0155(4). This disorder is only detectable for the most electron-rich atoms Au1 and Au2. The bond lengths and angles involving Au1 or Au2 are comparable.

Complex **8** was subsequently involved in cyclometallation in the same way as described for the monophosphane ligand **L1**H, with $[MCp^*Cl_2]_2$ (M = Rh or Ir, Cp* = C_5Me_5) and excess of NaOAc. The resulting complexes **9** (M = Rh) and **10** (M = Ir) were fully characterised, including single crystal structure determinations (Fig. 4). The gold–rhodium complex **9** crystallised in the monoclinic space group $P2_1/c$, the gold–iridium complex **10** in the triclinic space group $P\bar{1}$. Selected bond lengths and angles of **8**, **9**, and **10** are given in Table S5.† Further crystallographic details for these complexes are given in Table S1 (ESI†).

Finally, to obtain a complex with a more easily accessible active site, an anion exchange reaction was performed for complex **10** with $AgNTf_2$ in acetonitrile. The formation of **11** was confirmed *in situ* with multinuclear NMR spectroscopic analysis. The exchange of the Cl anion with NTf_2 led to a downfield shift of the phosphorus signals in the ^{31}P NMR spectrum and a smaller P,P coupling constant.

Catalytic activity

Allenyl ether rearrangement. The catalytic activity of complexes **7** and **11** in the allenyl ether rearrangement shown in Scheme 2 was investigated in an NMR tube in the presence of 1 equiv. 1,4-dinitrobenzene and CD_2Cl_2 as solvent. The reaction mixture was cooled to 0 °C, and then 0.5 mol% of catalyst **7** or **11** (prepared *in situ*) was added. The reaction was followed by ^{1}H NMR spectroscopy. After 1 h at 0 °C, partial conversion of the starting material induced by catalyst **7** based on the monophosphane ligand **L1** was observed, while catalyst **11** based on the triphosphane ligand **L2** was inactive. These results corroborate the importance of the environment around the metal centre for catalytic activity. Au^I is catalytically active only if it has a free coordination site, whilst the tridentate ligand renders gold(I) catalytically inactive.

With **7** as catalyst, the consumption of the starting material increased by increasing the temperature from 0 °C to room temperature. However, the conversion was still incomplete after 14.5 h at room temperature. Additionally, besides the desired aldehyde, the formation of a side product was observed. Although we did not investigate the nature and origin of the side product, based on previous reports in the literature, this is presumably the hydrolysis product as hydrolysis is described as a side reaction observed for some combinations of ligands with weakly coordinating counterions. Hashmi *et al.*[43] managed to avoid hydrolysis in this transform-

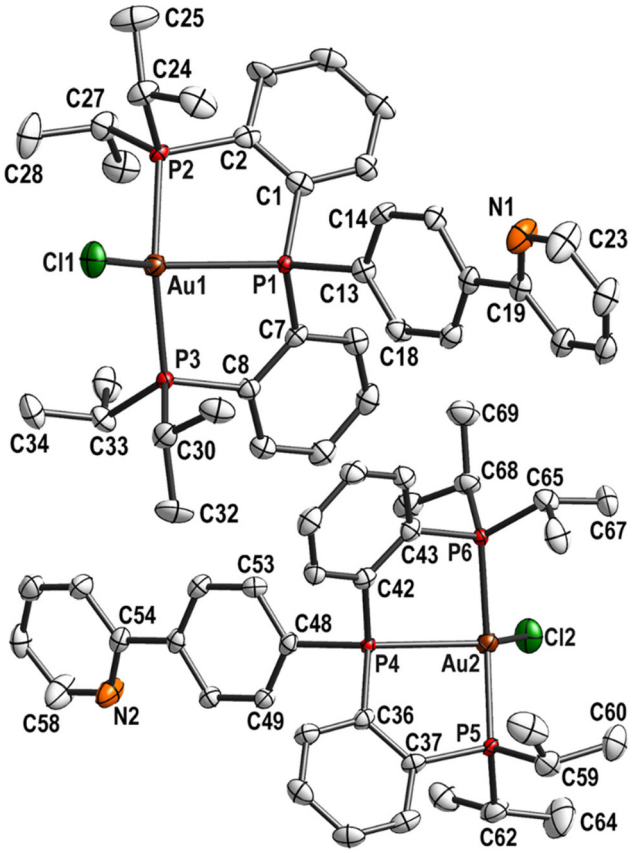

Fig. 3 Molecular structure and labelling scheme of **8**. Both independent molecules are shown. Hydrogen atoms are omitted for clarity and displacement ellipsoids are drawn at the 50% probability level.

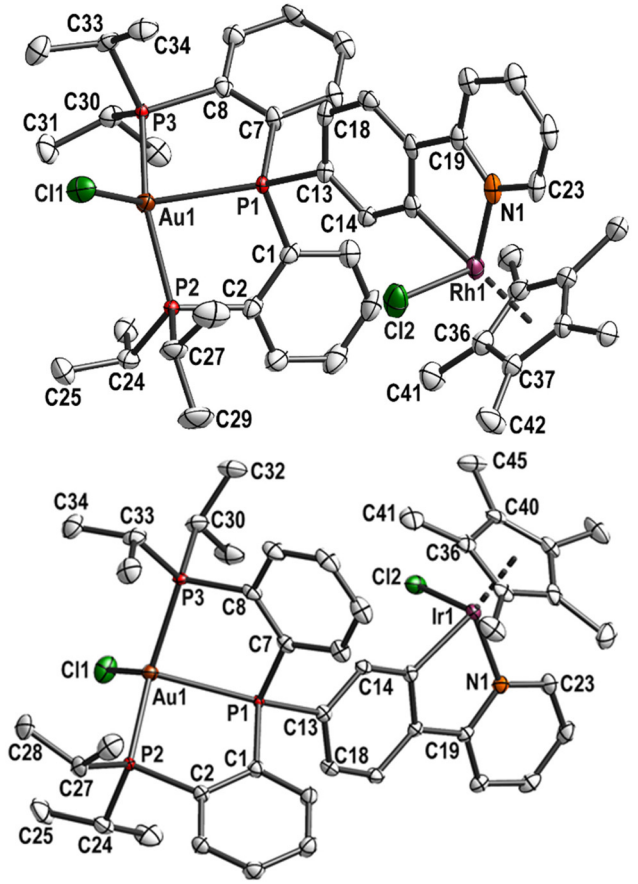

Fig. 4 Molecular structure and labelling scheme of **9** (top) and **10** (bottom). Hydrogen atoms are omitted for clarity and displacement ellipsoids are drawn at the 50% probability level.

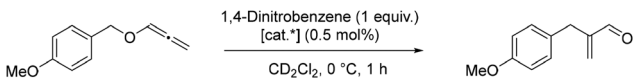

Scheme 2 Allenyl ether rearrangement. [cat*] = complex **7** or **11**.

ation by using the isolated catalyst $[Au(PPh_3)]NTf_2$ instead of a mixture of $[AuCl(PPh_3)]$ (2 mol%) and $AgNTf_2$ (5 mol%), a combination first reported by Ramana *et al.*[45] The same group proposed the mechanism for the gold(I) catalysed [1,3] O→C rearrangement of allenyl ethers.[46] Thus, the reaction proceeds *via* the initial coordination of the oxygen of the allenyl ether to gold(I), leading to the elongation of the carbinol C–O bond. In case of sufficient electrophilicity of the oxygen substituent, the C–O bond is cleaved, leading to the formation of a contact-ion that subsequently undergoes the [1,3]-rearrangement.[46]

Cycloisomerisation of *N*-propargyl benzamide. Uncovered by Hashmi and co-workers in 2004,[47] the catalytic synthesis of oxazolines has quickly developed into a standard reaction for gold(I) complexes. Some vinylgold intermediates have been characterised and reported by Ahn *et al.*[48] In a theoretical study, Liu *et al.*[49] have provided new insights. Thus, the

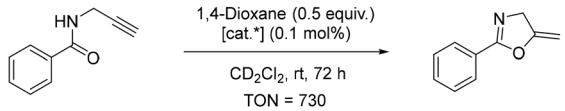

Scheme 3 Cycloisomerisation of *N*-propargyl benzamide. [cat*] = complex **7** or **11**.

gold(I)-catalysed 5-*exo-dig* ring-closing isomerisation of *N*-(2-propyn-1-yl)benzamide to 5-methylene-2-phenyl-4,5-dihydrooxazole was studied with complexes **7** and **11** in an NMR tube at room temperature in the presence of 0.5 equiv. 1,4-dioxane and CD_2Cl_2 as solvent (Scheme 3). The catalyst loading was 0.1 mol% of the corresponding complex **7** or **11**. The reaction was monitored by ^1H NMR spectroscopy. Similarly, as found for the allenyl ether rearrangement, complex **11** was catalytically inactive as it was unable to induce the cycloisomerisation.

On the other hand, complex **7** as a catalyst led to the complete conversion of the starting material within 72 hours. The turnover number (TON) of **7** was calculated after 24 h to be 730, comparable to the complex $[Au(P^tBu_3)]NTf_2$ with TON = 590.[43] Other gold(I) catalysts have also demonstrated the capacity to induce cycloisomerisation. Zuccaccia *et al.*[50] have even demonstrated that a range of NHC–Au–X [NHC = (1,3-bis(2,6-diisopropylphenyl)-imidazol-2-ylidene); X^- = BF_4^-, OTf^-, OTs^-, TFA^-] catalysts could induce the cycloisomerisation in a wide set of green solvents (cyclohexanone, isopropyl acetate, ethyl acetate, furfuryl alcohol, γ-valerolactone, propylene carbonate and propionic acid) in a comparable or better manner with respect to traditional volatile organic solvents. Furthermore, the catalyst activity is related to the basic strength of the anion, and the performances of the catalysts decrease gradually with increasing basicity and hydrogen-bond acceptor power of X^-. Kinetic experiments and DFT calculations conducted indicate that both the characteristics of the solvent and counterion should be taken into account.[50]

After the successful cycloisomerisation induced by **7**, 2 equiv. of $HSiEt_3$ were added to the same NMR tube to test if the heterobimetallic complex **7** can facilitate tandem catalysis. However, no reaction was observed within 22 h. When an additional amount of **7** was added (0.9 mol%), a grey precipitate formed, indicating the decomposition of the catalyst.

Conclusions

Heterobimetallic complexes Au/M (M = Rh^{III}, Ir^{III}) were synthesised using two ditopic ligands, namely a monophosphane **L1**H and a triphosphane **L2**H, and fully characterised, including single-crystal X-ray diffraction analyses for most complexes. The catalytic activity of cationic **7** (**L1**/Au^I/Ir^{III}) and **11** (**L2**/Au^I/Ir^{III}) in allenyl ether rearrangement and cycloisomerisation of *N*-propargyl benzamide was studied. While **7** showed some ability to induce allenyl ether rearrangement, **11** did not facilitate any conversion. Likewise, *N*-propargyl benzamide was con-

verted to oxazole in the presence of **7**, but no reaction was observed when **11** was used as a catalyst. These results demonstrate the importance of the metal centre's coordination sphere in catalytic processes.[20–22] Gold(I) is only catalytically active when coordinated by a monophosphane ligand, while the tridentate ligand led to loss of catalytic activity. Furthermore, while the gold(I) centre in cationic complex **7** was catalytically active, the second metal (Ir^{III}) could not be involved in tandem catalysis under the conditions reported here. More importantly, we demonstrated the universality of the ligand framework for designing heterobimetallic catalysts for future catalytic applications.

Experimental

Materials and methods

Reactions were performed using standard Schlenk line techniques. Reagents were purchased from chemical vendors and used without further purification unless noted otherwise. PCl_3 was degassed, distilled, and stored under a nitrogen atmosphere over 4 Å molecular sieves prior to use. $[RhCp^*Cl_2]_2$, $[IrCp^*Cl_2]_2$ ($Cp^* = C_5Me_5$),[23] P^iPr_2Cl,[24] and the triphosphane ligand bis[2-(diisopropylphosphanyl)phenyl]-4-(2-pyridyl)phenylphosphane (**L2H**)[20] were synthesised according to literature procedures. All other compounds are commercially available. NMR spectra were recorded at 25 °C with a Bruker AVANCE DRX 400 spectrometer (^{1}H NMR: 400.13 MHz, ^{13}C NMR: 100.16 MHz, ^{31}P NMR: 161.97 MHz). TMS was used as the internal standard for ^{1}H and ^{13}C NMR spectra; spectra of other nuclei were referenced to TMS. Mass spectra (HR-ESI-MS) were recorded on an FT-ICR-MS Bruker–Daltonics ESI mass spectrometer (APEX II, 7 T). Elemental analyses were carried out with a Heraeus VARIO EL oven. IR spectra were measured between 4000 and 400 cm^{-1} as KBr pellets on an FT-IR Spectrum 2000 spectrometer by PerkinElmer. All solvents were purified and degassed with an MBRAUN Solvent Purification System SPS-800. Dichloromethane (DCM) was stored under nitrogen over 4 Å molecular sieves. Tetrahydrofuran (THF) was distilled over K and benzophenone under nitrogen atmosphere and stored over 4 Å molecular sieves. Acetonitrile (ACN) was dried over P_2O_5 for 3 d, distilled over P_2O_5, and stored under N_2 atmosphere and over 3 Å molecular sieves. All deuterated solvents ($CDCl_3$, CD_2Cl_2, CD_3CN) were dried over 3 Å molecular sieves, degassed, and stored under N_2 atmosphere over 3 Å molecular sieves. Crystallographic data were collected on a Gemini diffractometer (Rigaku Oxford Diffraction) using Mo-Kα radiation and ω-scan rotation. Data reduction was performed with CrysAlisPro,[25] including the program SCALE3 ABSPACK for an empirical absorption correction. With the exception of structures **L1H**, **1**, and **3**, an additional analytical numeric absorption correction was applied using a multifaceted crystal model based on expressions derived by Clark and Reid.[26] All structures were solved by dual space methods with SHELXT[27] and refined with SHELXL.[28] Non-hydrogen atoms were refined with anisotropic displacement parameters. For **L1H**, hydrogen atoms were located with a difference-density Fourier map. For all other structures, hydrogen atoms were calculated on idealised positions using the riding model. Structure figures were generated with DIAMOND-4.[29]

CCDC deposition numbers given in Table S1 in the ESI† contain the supplementary crystallographic data for this paper.

Synthesis of monophosphane sulfide ligand L1H

2-(4-Bromophenyl)pyridine (2.483 g, 10.6 mmol, 1.05 equiv.) was dissolved in THF (30 ml) and cooled to −60 °C. To the cooled solution, *n*BuLi in Et_2O (8.0 ml, 11.1 mmol, 1.1 equiv.) was added dropwise, and the reaction mixture was stirred for one hour. Diisopropylchlorophosphane (1.54 g, 10.1 mmol, 1.0 equiv.) was dissolved in Et_2O, cooled to −60 °C and added dropwise to the lithiated 2-phenylpyridine. The reaction mixture was left to warm up to room temperature overnight. Water (30 ml) was added to the solution, the layers were separated, and the organic layer was washed with water (2 × 10 ml) and brine (10 ml). The aqueous layers were extracted with DCM (3 × 10 ml), and the combined organic layers were dried over $MgSO_4$. The solvent was removed, resulting in a yellow oil. The pure monophosphane ligand was obtained upon column chromatography with *n*-hexane containing a gradually increasing amount of ethyl acetate (5–10%). The monophosphane ligand (1.153 g, 4.25 mmol, 1 equiv.) was dissolved in THF (5 ml). S_8 (0.136 g, 4.25 mmol, 1 equiv.) and a catalytic amount of NEt_3 (1 drop) was added, and the reaction mixture was stirred at 50 °C for 24 h. Pure monophosphane sulfide **L1H** was obtained upon column chromatography with *n*-hexane containing a gradually decreasing amount of ethyl acetate (40–10%). Colourless single crystals (prisms) of **L1H** were obtained by slow solvent evaporation from a saturated DCM/Et_2O solution. Yield: 1.13 g (88%).

^{1}H NMR (400.1 MHz, $CDCl_3$): δ = 1.09 (dd, $^3J_{HP}$ = 17 Hz, $^3J_{HH}$ = 7.0 Hz, 6 H, 2″-H), 1.24 (dd, $^3J_{HP}$ = 17 Hz, $^3J_{HH}$ = 7.0 Hz, 6 H, 4″-H), 2.55 (heptd, $^3J_{HH}$ = 7.0 Hz, J_{HP} = 1.3 Hz, 2 H, 1″ and 3″-H), 7.31 (tt, $^3J_{HH}$ = 8.0 Hz, $^4J_{HH}$ = 1.7 Hz, 1 H, 2′-H), 7.81 (m, $^3J_{HH}$ = 8.0 Hz, $^3J_{HH}$ = 5.0 Hz, $^4J_{HH}$ = 1.7 Hz, 2 H, 3′ and 4′-H), 7.97 (m, $^3J_{HH}$ = 8.0 Hz, $^4J_{HH}$ = 2.3 Hz, 2 H, 2-H), 8.11 (dd, $^3J_{HH}$ = 8.0 Hz, $^4J_{HH}$ = 2.3 Hz, 2 H, 3-H), 8.74 (dt, $^3J_{HH}$ = 5.0 Hz, $^4J_{HH}$ = 1.4 Hz, 1 H, 5′-H) ppm. $^{13}C\{^1H\}$ NMR (100.6 MHz, $CDCl_3$): δ = 15.7 (s, C2″), 16.5 (s, C4″), 27.6 (d, $^1J_{CP}$ = 51 Hz, C1″ and C3″), 121.0 (s, 3′), 122.9 (s, C2′), 126.6 (d, $^3J_{CP}$ = 11 Hz, C3), 132.6 (d, $^2J_{CP}$ = 8.5 Hz, C2), 137.2 (s, C4′), 141.9 (s, C1), 149.6 (s, C5′), 156.1 (s, C1′) ppm. $^{31}P\{^1H\}$ NMR (161.97 MHz, $CDCl_3$): δ = 66.4 ppm.

HR-MS (CH_3OH): ($C_{17}H_{22}NPS$; $[M + H]^+$, pos. ESI) calcd: 304.1283, found: 304.1281.

Synthesis of complexes 1 and 2

Monophosphane sulfide **L1H** (61 mg, 0.2 mmol, 1 equiv.) was dissolved in DCM or ACN (for reactions with M = Rh and Ir, respectively). $[MCp^*Cl_2]_2$ (M = Rh, Ir; 0.1 mmol, 0.5 equiv.) and anhydrous NaOAc (49 mg, 0.6 mmol, 3 equiv.) were added, and the reaction mixture was stirred at room temperature or

50 °C (for reactions with M = Rh and Ir, respectively). Single crystals of **1** (orange plates) were obtained by slow cooling of a saturated solution in MeOH, while for **2**, obtained as orange prisms, a saturated solution in ACN was used.

1: Yield: 114.6 mg (97%).

^{1}H NMR (400.1 MHz, $CDCl_3$): δ = 1.12 (dd, $^3J_{HP}$ = 10 Hz, $^3J_{HH}$ = 7.0 Hz, 3 H, 2″-H), 1.16 (dd, $^3J_{HP}$ = 10 Hz, $^3J_{HH}$ = 7.0 Hz, 3 H, 3″-H), 1.21 (dd, $^3J_{HP}$ = 17 Hz, $^3J_{HH}$ = 7.0 Hz, 3 H, 5″-H), 1.31 (dd, $^3J_{HP}$ = 17 Hz, $^3J_{HH}$ = 7.0 Hz, 3 H, 6″-H), 1.66 (s, 15 H, Cp*–Me), 2.50 (heptd, $^3J_{HH}$ = 7.0 Hz, $^2J_{HP}$ = 1.3 Hz, 1 H, 1″-H), 2.59 (heptd, $^3J_{HH}$ = 7.0 Hz, $^2J_{HP}$ = 1.3 Hz, 1 H, 4″-H), 7.22 (m, $^3J_{HH}$ = 6.4 Hz, $^4J_{HH}$ = 1.6 Hz, 1 H, 4′-H), 7.56 (m, $^3J_{HH}$ = 8.0 Hz, $^4J_{HH}$ = 1.5 Hz, 1 H, 6-H), 7.68 (dd, $^3J_{HH}$ = 8.0 Hz, $^4J_{HH}$ = 2.6 Hz, 1 H, 5-H), 7.77 (m, $^3J_{HH}$ = 8.0 Hz, $^4J_{HH}$ = 1.6 Hz, 1 H, 3′-H), 7.85 (dt, $^3J_{HH}$ = 8.0 Hz, $^4J_{HH}$ = 1.2 Hz, 1 H, 2′-H), 8.31 (dd, $^3J_{HH}$ = 8.0 Hz, $^4J_{HH}$ = 1.5 Hz, 1 H, 2-H), 8.79 (dt, $^3J_{HH}$ = 6.4 Hz, $^4J_{HH}$ = 1.0 Hz, 1 H, 5′-H) ppm. ^{13}C{^{1}H} NMR (100.6 MHz, $CDCl_3$): δ = 9.3 (s, Cp*–Me), 16.0 (s, C2″ and C3″), 16.8 (t, $^2J_{CP}$ = 2.6 Hz, C5″ and C6″), 27.7 (d, $^1J_{CP}$ = 51 Hz, C1″), 28.2 (d, $^1J_{CP}$ = 51 Hz, C4″), 96.3 (d, $^1J_{CRh}$ = 6.3 Hz, Cp*), 119.9 (s, C2′), 122.6 (s, C4′), 122.9 (s, C5), 126.6 (d, $^2J_{CP}$ = 9.3 Hz, C6), 128.4 (d, C4), 137.3 (s, C3′), 140.5 (d, $^2J_{CP}$ = 6.3 Hz, C2), 146.5 (d, $^1J_{CP}$ = 2.7 Hz, C1), 151.4 (s, C5′), 164.4 (s, C1′), 178.1 (dd, $^1J_{CRh}$ = 32.5 Hz, $^3J_{CP}$ = 8.4 Hz C3) ppm. ^{31}P{^{1}H} NMR (161.97 MHz, $CDCl_3$): δ = 67.0 ppm.

Elemental analysis for $C_{27}H_{36}ClNPRhS$ calcd: C 56.30, H 6.30, N 2.43, found: C 55.11, H 5.52, N 2.32.

2: Yield: 131.9 mg (97%).

^{1}H NMR (400.1 MHz, $CDCl_3$): δ = 1.12 (dd, $^3J_{HP}$ = 13 Hz, $^3J_{HH}$ = 7.0 Hz, 3 H, 2″-H), 1.16 (dd, $^3J_{HP}$ = 13 Hz, $^3J_{HH}$ = 7.0 Hz, 3 H, 3″-H), 1.21 (dd, $^3J_{HP}$ = 17 Hz, $^3J_{HH}$ = 7.0 Hz, 3 H, 5″-H), 1.30 (dd, $^3J_{HP}$ = 17 Hz, $^3J_{HH}$ = 7.0 Hz, 3 H, 6″-H), 1.70 (s, 15 H, Cp*–Me), 2.48 (heptd, $^3J_{HH}$ = 7.0 Hz, 1 H, 1″-H), 2.59 (heptd, $^3J_{HH}$ = 7.0 Hz, 1 H, 4″-H), 7.16 (m, $^3J_{HH}$ = 6.5 Hz, $^4J_{HH}$ = 1.4 Hz, 1 H, 4′-H), 7.52 (m, $^3J_{HH}$ = 10.0 Hz, $^4J_{HH}$ = 1.5 Hz, 1 H, 6-H), 7.73 (m, $^3J_{HH}$ = 10.0, $^3J_{HH}$ = 8.0 Hz, $^4J_{HH}$ = 2.6 Hz, 2 H, 5-H and 3′-H), 7.90 (d, $^3J_{HH}$ = 8.0 Hz, 1 H, 2′-H), 8.31 (dd, $^3J_{HH}$ 11.2 Hz, $^4J_{HH}$ = 1.5 Hz, 1 H, 2-H), 8.74 (dd, $^3J_{HH}$ = 6.5 Hz, $^4J_{HH}$ = 1.3 Hz, 1 H, 5′-H) ppm. ^{13}C{^{1}H} NMR (100.6 MHz, $CDCl_3$): δ = 9.2 (s, Cp*–Me), 16.2 (s, C2″ and C3″), 17.0 (s, C5″ and C6″), 27.7 (d, $^1J_{CP}$ = 50.5 Hz, C1″), 28.5 (d, $^1J_{CP}$ = 50.5 Hz, C4″), 89.1 (s, Cp*), 119.9 (s, C2′), 123.2 (d, $^3J_{CP}$ = 11.7 Hz, C5), 123.5 (s, C4′), 125.9 (d, $^2J_{CP}$ = 9.4 Hz, C6), 128.8 (s, C6′), 129.5 (s, C3′), 137.4 (s, $^2J_{CP}$ = 6.3 Hz, C2), 139.8 (d, $^1J_{CP}$ = 7.8 Hz, C1), 147.3 (d, $^4J_{CP}$ = 2.7 Hz, C4), 151.7 (s, C5′), 163.0 (d, $^3J_{CP}$ = 8.8 Hz C3), 166.4 (s, C1′) ppm. ^{31}P{^{1}H} NMR (161.97 MHz, $CDCl_3$): δ = 66.7 ppm.

HR-MS (CH_3OH): ($C_{27}H_{36}ClNPIrS$; [M − Cl]$^+$, pos. ESI) calcd: 630.1929, found: 630.1920.

Desulfurisation reaction: preparation of 3 and 4

Complex **1** (25 mg, 0.434 mmol) was dissolved in THF (4 ml). Freshly activated RANEY®-Ni was added, and the reaction mixture was heated to 50 °C. The progress of the reaction was monitored with ^{31}P{^{1}H} NMR, and if necessary, small amounts of activated RANEY®-Ni were added until conversion was complete.

Yield: 145.3 mg (60%), orange prisms.

^{1}H NMR (400.1 MHz, $CDCl_3$): δ = 1.02 (dd, $^3J_{HP}$ = 10 Hz, $^3J_{HH}$ = 7.0 Hz, 3 H, 2″-H), 1.03 (dd, $^3J_{HP}$ = 10 Hz, $^3J_{HH}$ = 7.0 Hz, 3 H, 3″-H), 1.12 (dd, $^3J_{HP}$ = 15 Hz, $^3J_{HH}$ = 7.0 Hz, 3 H, 5″-H), 1.18 (dd, $^3J_{HP}$ = 15 Hz, $^3J_{HH}$ = 7.0 Hz, 3 H, 6″-H), 1.64 (s, 15 H, Cp*–Me), 2.14 (heptd, $^3J_{HH}$ = 7.0 Hz, J_{HP} = 1.2 Hz, 1 H, 1″-H), 2.23 (heptd, $^3J_{HH}$ = 7.0 Hz, J_{HP} = 3.2 Hz, 1 H, 4″-H), 7.14 (tt, $^3J_{HH}$ = 8.0 Hz, $^4J_{HH}$ = 1.4 Hz, 1 H, 4′-H), 7.19 (tt, $^3J_{HH}$ = 8.0 Hz, $^4J_{HH}$ = 1.5 Hz, 1 H, 6-H), 7.57 (d, $^3J_{HH}$ = 8.0 Hz, 1 H, 5-H), 7.71 (td, $^3J_{HH}$ = 8.0 Hz, $^4J_{HH}$ = 1.6 Hz, 1 H, 3′-H), 7.78 (dt, $^3J_{HH}$ = 8.0 Hz, $^4J_{HH}$ = 1.2 Hz, 1 H, 2′-H), 7.94 (dd, $^3J_{HH}$ = 6.8 Hz, $^4J_{HH}$ = 1.4 Hz, 1 H, 2-H), 8.75 (dt, $^3J_{HH}$ = 5.5 Hz, $^4J_{HH}$ = 1.0 Hz, 1 H, 5′-H) ppm. ^{13}C{^{1}H} NMR (100.6 MHz, $CDCl_3$): δ = 9.2 (s, Cp*–Me), 18.8 (d, $^2J_{CP}$ = 7.0 Hz, C2″), 19.5 (d, $^2J_{CP}$ = 10.0 Hz, C3″), 20.0 (d, $^2J_{CP}$ = 18.6 Hz, C5″), 20.2 (d, $^2J_{CP}$ = 18.6 Hz, C6″), 23.2 (d, $^1J_{CP}$ = 12 Hz, C1″), 23.3 (d, $^1J_{CP}$ = 12 Hz, C4″), 96.0 (d, $^1J_{CRh}$ = 6.3 Hz, Cp*), 119.3 (s, C2′), 122.1 (s, C4′), 122.5 (d, $^3J_{CP}$ = 8.0 Hz, C5), 129.2 (d, $^2J_{CP}$ = 20.0 Hz, C6), 137.0 (s, C3′), 137.2 (s, C4), 142.8 (d, $^2J_{CP}$ = 7.1 Hz, C2), 144.2 (s, C1), 151.2 (s, C5′), 165.2 (s, C1′), 177.7 (dd, $^1J_{CRh}$ = 32.2 Hz, $^3J_{CP}$ = 5.7 Hz, C3) ppm. ^{31}P{^{1}H} NMR (161.97 MHz, $CDCl_3$): δ = 13.7 ppm.

HR-MS (CH_3OH): ($C_{27}H_{36}ClNPRh$; pos. ESI) calcd for [M − Cl]$^+$: 508.1635, found: 508.1646.

Complex **4** (0.434 mmol, dissolved in THF (4 ml)) was prepared in the same way as complex **3**, but was directly used in the next step to give complex **6**.

Synthesis of heterobimetallic complexes 5 and 6

Free phosphane compound **3** or **4** (120 mg or 135 mg, respectively, 0.21 mmol, 1 equiv.) was dissolved in DCM and reacted with [AuCl(tht)] (68 mg, 0.21 mmol, 1 equiv.) at room temperature for 15 min to afford precipitated heterobimetallic complexes **5** (M = Rh, orange prisms) and **6** (M = Ir, orange prisms) quantitatively.

5: ^{1}H NMR (400.1 MHz, CD_2Cl_2): δ = 1.06 (dd, $^3J_{HP}$ = 13 Hz, $^3J_{HH}$ = 7.0 Hz, 3 H, 2″-H), 1.10 (dd, $^3J_{HP}$ = 13 Hz, $^3J_{HH}$ = 7.0 Hz, 3 H, 3″-H), 1.20 (dd, $^3J_{HP}$ = 17 Hz, $^3J_{HH}$ = 7.0 Hz, 3 H, 5″-H), 1.25 (dd, $^3J_{HP}$ = 17 Hz, $^3J_{HH}$ = 7.0 Hz, 3 H, 6″-H), 1.56 (s, 15 H, Cp*–Me), 2.49 (heptd, $^3J_{HH}$ = 7.0 Hz, $^2J_{HP}$ = 1.7 Hz, 2 H, 1″ and 4″-H), 7.21 (tt, $^3J_{HH}$ = 6.4 Hz, $^4J_{HH}$ = 1.7 Hz, 1 H, 4′-H), 7.28 (tt, $^3J_{HH}$ = 9.0 Hz, $^4J_{HH}$ = 1.7 Hz, 1 H, 6-H), 7.64 (dd, $^3J_{HH}$ = 8.0 Hz, $^4J_{HH}$ = 2.2 Hz, 1 H, 5-H), 7.75 (td, $^3J_{HH}$ = 8.0 Hz, $^4J_{HH}$ = 1.5 Hz, 1 H, 3′-H), 7.81 (dt, $^3J_{HH}$ = 8.0 Hz, $^4J_{HH}$ = 1.2 Hz, 1 H, 2′-H), 8.14 (dd, $^3J_{HH}$ = 12.7 Hz, $^4J_{HH}$ = 1.6 Hz, 1 H, 2-H), 8.70 (dt, $^3J_{HH}$ = 5.5 Hz, $^4J_{HH}$ = 1.0 Hz, 1 H, 5′-H) ppm. ^{13}C{^{1}H} NMR (100.6 MHz, CD_2Cl_2): δ = 9.4 (s, Cp*–Me), 18.7 (d, $^2J_{CP}$ = 17.4 Hz, C2″ and C3″), 19.7 (d, $^2J_{CP}$ = 13.7 Hz, C5″ and C6″), 25.4 (d, $^1J_{CP}$ = 20.3 Hz, C1″), 25.7 (d, $^1J_{CP}$ = 19.8 Hz, C4″), 96.7 (d, $^1J_{CRh}$ = 6.3 Hz, Cp*), 120.3 (s, C2′), 123.2 (d, $^3J_{CP}$ = 10.4 Hz, C5), 123.7 (s, C4′), 126.5 (d, $^1J_{CP}$ = 49.0 Hz, C1), 128.3 (d, $^2J_{CP}$ = 10.3 Hz, C6), 137.9 (s, C3′), 144.9 (d, $^2J_{CP}$ = 12.9 Hz, C2), 147.9 (s, C4), 152.0 (s, C5′), 164.2 (s, C1′), 179.8 (dd, $^1J_{CRh}$ = 33.0 Hz, $^3J_{CP}$ = 9.1 Hz, C3) ppm. ^{31}P{^{1}H} NMR (161.97 MHz, CD_2Cl_2): δ = 60.5 ppm.

HR-MS (CH_3OH): ($C_{27}H_{36}AuCl_2NPRh$; [M − Cl]$^+$, pos. ESI) calcd: 740.0989, found: 740.0924.

6: ^{1}H NMR (400.1 MHz, $CDCl_3$): δ = 1.13 (dd, $^{3}J_{HP}$ = 10.0 Hz, $^{3}J_{HH}$ = 7.0 Hz, 3 H, 2″-H), 1.17 (dd, $^{3}J_{HP}$ = 10.0 Hz, $^{3}J_{HH}$ = 7.0 Hz, 3 H, 3″-H), 1.27 (dd, $^{3}J_{HP}$ = 18.6 Hz, $^{3}J_{HH}$ = 7.0 Hz, 3 H, 5″-H), 1.32 (dd, $^{3}J_{HP}$ = 18.6 Hz, $^{3}J_{HH}$ = 7.0 Hz, 3 H, 6″-H), 1.71 (s, 15 H, Cp*–Me), 2.52 (heptd, $^{3}J_{HH}$ = 7.0 Hz, $^{2}J_{HP}$ = 1.7 Hz, 2 H, 1″ and 4″-H), 7.19 (tt, $^{3}J_{HH}$ = 6.4 Hz, $^{4}J_{HH}$ = 1.5 Hz, 1 H, 4′-H), 7.30 (tt, $^{3}J_{HH}$ = 9.0 Hz, $^{4}J_{HH}$ = 1.7 Hz, 1 H, 6-H), 7.74 (m, $^{3}J_{HH}$ = 8.0 Hz, $^{4}J_{HH}$ = 1.5 Hz, 2 H, 5-H and 3′-H), 7.90 (d, $^{3}J_{HH}$ = 8.0 Hz, 1 H, 2′-H), 8.25 (dd, $^{3}J_{HH}$ = 13.0 Hz, $^{4}J_{HH}$ = 1.6 Hz, 1 H, 2-H), 8.76 (d, $^{3}J_{HH}$ = 5.5 Hz, 1 H, 5′-H) ppm. $^{13}C\{^{1}H\}$ NMR (100.6 MHz, $CDCl_3$): δ = 9.0 (s, Cp*–Me), 18.4 (d, $^{2}J_{CP}$ = 4.8 Hz, C2″ and C3″), 19.4 (d, $^{2}J_{CP}$ = 4.4 Hz, C5″ and C6″), 24.9 (d, $^{1}J_{CP}$ = 34.6 Hz, C1″), 25.3 (d, $^{1}J_{CP}$ = 34.2 Hz, C4″), 89.0 (s, Cp*), 119.8 (s, C2′), 123.4 (d, $^{3}J_{CP}$ = 11.0 Hz, C5), 123.6 (s, C4′), 126.5 (d, $^{1}J_{CP}$ = 50.0 Hz, C3), 127.2 (d, $^{2}J_{CP}$ = 10.7 Hz, C6), 137.3 (s, C3′), 143.5 (d, $^{2}J_{CP}$ = 12.9 Hz, C2), 147.9 (s, C4), 151.6 (s, C5′), 164.0 (d, $^{3}J_{CP}$ = 9.7 Hz, C1), 165.9 (s, C1′) ppm. $^{31}P\{^{1}H\}$ NMR (161.97 MHz, $CDCl_3$): δ = 60.0 ppm.

HR-MS (CH_3OH): ($C_{27}H_{36}AuCl_2IrNP$; $[M - Cl]^+$, pos. ESI) calcd: 830.1556, found: 830.1559.

Elemental analysis for $C_{27}H_{36}AuCl_2IrNP$ calcd: C 37.46, H 4.19, N 1.62, found: C 37.78, H 3.84, N 1.58.

Anion exchange reaction: preparation of 7

Complex **6** (17.3 mg, 0.02 mmol, 1 equiv.) was dissolved in CD_2Cl_2 (1 ml) and CD_3CN (1 ml). $AgNTf_2$ (15.5 mg, 0.04 mmol, 2 equiv.) was added, and the reaction mixture was stirred at room temperature for 15 min. The precipitate (AgCl) was filtered off, and the filtrate was analysed *in situ*.

^{1}H NMR (400.1 MHz, CD_3CN/CD_2Cl_2): δ = 1.12 (dd, $^{3}J_{HP}$ = 6.0 Hz, $^{3}J_{HH}$ = 7.0 Hz, 3 H, 2″-H), 1.13 (dd, $^{3}J_{HP}$ = 6.0 Hz, $^{3}J_{HH}$ = 7.0 Hz, 3 H, 3″-H), 1.28 (dd, $^{3}J_{HP}$ = 19.0 Hz, $^{3}J_{HH}$ = 7.0 Hz, 3 H, 5″-H), 1.31 (dd, $^{3}J_{HP}$ = 19.0 Hz, $^{3}J_{HH}$ = 7.0 Hz, 3 H, 6″-H), 1.72 (s, 15 H, Cp*–Me), 2.66 (heptd, $^{3}J_{HH}$ = 7.0 Hz, 2 H, 1″ and 4″-H), 7.43 (m, $^{3}J_{HH}$ = 5.7 Hz, $^{4}J_{HH}$ = 1.5 Hz, 1 H, 4′-H), 7.46 (m, $^{3}J_{HH}$ = 8.0 Hz, $^{4}J_{HH}$ = 1.6 Hz, 1 H, 4′-H), 7.90 (dd, $^{3}J_{HH}$ = 8.0 Hz, $^{4}J_{HH}$ = 2.3 Hz, 1 H, 6-H), 8.00 (td, $^{3}J_{HH}$ = 8.0 Hz, $^{4}J_{HH}$ = 1.5 Hz, 1 H, 3′-H), 8.10 (dt, $^{3}J_{HH}$ = 8.0 Hz, $^{4}J_{HH}$ = 1.2 Hz, 1 H, 2′-H), 8.31 (dd, $^{3}J_{HH}$ = 13.5 Hz, $^{4}J_{HH}$ = 1.6 Hz, 1 H, 2-H), 8.76 (d, $^{3}J_{HH}$ = 5.7 Hz, $^{4}J_{HH}$ = 0.7 Hz, 1 H, 5′-H) ppm. $^{13}C\{^{1}H\}$ NMR (100.6 MHz, CD_3CN/CD_2Cl_2): δ = 9.0 (s, Cp*–Me), 18.8 (d, $^{2}J_{CP}$ = 6.0 Hz, C2″ and C3″), 19.8 (d, $^{2}J_{CP}$ = 2.0 Hz, C5″ and C6″), 25.6 (d, $^{1}J_{CP}$ = 35.0 Hz, C1″), 25.7 (d, $^{1}J_{CP}$ = 35.0 Hz, C4″), 92.3 (s, Cp*), 119.0 (s, C–NTf_2), 121.5 (s, C2′), 122.2 (s, C1), 124.9 (d, $^{1}J_{CP}$ = 10.0 Hz, C6), 125.8 (s, C4′), 129.0 (d, $^{2}J_{CP}$ = 12.9 Hz, C2), 140.4 (s, C3′), 144.8 (d, $^{3}J_{CP}$ = 4.0 Hz, C5), 149.6 (s, C4), 153.3 (s, C5′), 157.5 (d, $^{3}J_{CP}$ = 6.6 Hz, C3), 165.9 (s, C1′) ppm. $^{31}P\{^{1}H\}$ NMR (161.97 MHz, CD_3CN/CD_2Cl_2): δ = 61.6 ppm.

HR-MS (CD_3CN/CD_2Cl_2): ($C_{31}H_{36}AuF_{12}IrN_3O_8PS_4$; $[M - NTf_2]^+$, pos. ESI) calcd: 1075.1046, found: 1075.1053.

Synthesis of 8

The triphosphane ligand **L2H** (0.578 g, 1.01 mmol, 1 equiv.) was dissolved in DCM (20 ml) and [AuCl(tht)] (0.324 g, 1.01 mmol, 1 equiv.) was added, resulting in a colour change to deep red. The solution was stirred for 1 h; then, all volatile compounds were removed *in vacuo*. The product was obtained quantitatively after recrystallisation from a mixture of 10 ml DCM and 50 ml *n*-hexane and washing with *n*-pentane. The compound is not light-sensitive and can be stored in a DCM solution for weeks. Single crystals (orange prisms) suitable for X-ray diffraction could be obtained by dissolving 10 mg in DCM and layering with *n*-hexane.

^{1}H NMR (400.1 MHz, $CDCl_3$): δ = 8.66 (d, $^{3}J_{HH}$ = 4.8 Hz, 1 H, 5′-H), 8.02–7.94 (m, 2 H, 6″-H), 7.81 (dd, $^{3}J_{HH}$ = 8.4, $^{4}J_{PH}$ = 2.1 Hz, 2 H, 3-H), 7.74 (td, $^{3}J_{HH}$ = 7.7, $^{4}J_{HH}$ = 1.9 Hz, 1 H, 3′-H), 7.67 (d, $^{3}J_{HH}$ = 7.9 Hz, 1 H, 2′-H), 7.64–7.60 (m, 2 H, 3″-H), 7.49 (*pseudo* p, *N* = 7.2 Hz, 4 H, 4″- and 5″-H), 7.22 (dd, $^{3}J_{HH}$ = 7.3, 5.0 Hz, 1 H, 4′-H), 7.06 (dd, $^{3}J_{HH}$ = 8.3, $^{3}J_{PH}$ = 6.6 Hz, 2 H, 2-H), 2.84–2.64 (m, 4 H, 1‴-H), 1.50–1.41 (m, 6 H, 2‴-H), 1.37 (*pseudo* q, $^{3}J_{HH/HP}$ = 8.1 Hz, 6 H, 2‴-H), 1.25 (*pseudo* q, $^{3}J_{HH/HP}$ = 6.9 Hz, 6 H, 2‴-H), 0.82 (*pseudo* dt, $^{3}J_{PH}$ = 9.3 Hz, $^{3}J_{HH}$ = 6.9 Hz, 6 H, 2‴-H) ppm. $^{13}C\{^{1}H\}$ NMR (100.6 MHz, $CDCl_3$): δ = 156.7 (C1′), 149.5 (C5′), 145.3 (*pseudo* q, $^{1}J_{CP}$ = 12.5 Hz, C2″), 142.3 (C1) 138.4 (m, C4/C1″), 137.0 (C3′), 135.9 (C6″), 131.9 (m, C2/C3″), 130.7 (C4″), 129.8 (C5″), 126.8 (d, $^{4}J_{CP}$ = 4.6 Hz, C3), 122.2 (C4′), 120.6 (C2′), 27.2 (*pseudo* t, $^{1}J_{CP}$ = 13.3 Hz, C1‴), 23.6 (m, C1‴), 20.0 (m, C2‴), 19.8 (m, C2‴), 19.1 (C2‴), 17.0 (C2‴) ppm. $^{31}P\{^{1}H\}$ NMR (161.97 MHz, $CDCl_3$): δ = 58.3 (d, $^{2}J_{PP}$ = 114.8 Hz, 2 P, $P_{terminal}$), −5.0 (t, $^{2}J_{PP}$ = 114.4 Hz, 1 P, $P_{central}$) ppm.

HR-MS (CH_3OH): ($C_{35}H_{44}AuClNP_3$; $[M - Cl]^+$, pos. ESI) calcd: 768.2347 found: 768.2299.

Synthesis of heterobimetallic complexes 9 and 10

The gold complex **8** (0.5 mmol, 2 equiv.) was suspended in ACN (30 ml) together with $[Cp^*MCl_2]_2$ (M = Rh or Ir, 0.25 mmol, 1 equiv.) and NaOAc (1.5 mmol, 6 equiv.) and stirred at room temperature for 48 h. The suspension was filtered over Celite, and then extracted with DCM. Removal of the volatiles in high vacuum gave the product quantitatively. Single crystals (orange needles) suitable for X-ray diffraction could be obtained by layering a frozen DCM solution with *n*-hexane (**9**) or from a hot saturated solution in ACN (**10**).

9: ^{1}H NMR (400.1 MHz, CD_2Cl_2): δ = 8.69 (d, $^{3}J_{HH}$ = 5.6 Hz, 1 H, 5′-H), 8.19 (m, 1 H, 6″-H), 8.03 (m, 1 H, 6″-H), 7.75 (dd, $^{3}J_{HH}$ = 4.8 Hz, $^{4}J_{HH}$ = 1.1 Hz, 2 H, 2′- and 3′-H), 7.68 (m, 2 H, 3″-H), 7.65–7.60 (m, 2 H, 4″- and 5″-H), 7.58 (m, 2 H, 4″- and 5″-H), 7.50 (d, $^{3}J_{HH}$ = 8.1 Hz, 1 H, 5-H), 7.39 (d, $^{4}J_{HH}$ = 1.6 Hz, 1 H, 2-H), 7.21–7.17 (m, 1 H, 4′-H), 6.72 (dd, $^{3}J_{PH,HH}$ = 8.4 Hz, $^{4}J_{HH}$ = 1.7 Hz, 1 H, 6-H), 2.82 (m, 2 H, 1‴-H), 2.67 (m, 2 H, 1″′-H), 1.44 (m, 6 H, 2‴-H) 1.42 (s, 15 H, Cp*–Me), 1.36 (m, 6 H, 2‴-H), 1.28 (m, 6 H, 2‴-H), 0.83 (ddd, $^{3}J_{PH}$ = 18.1 Hz, $^{3}J_{HH}$ = 6.7, 4.6 Hz, 6 H, 2‴-H) ppm. $^{13}C\{^{1}H\}$ NMR (100.6 MHz, CD_2Cl_2): δ = 179.9 (d, $^{1}J_{RhC}$ = 33 Hz, C3), 164.8 (C1′), 151.9 (C5′), 145.2 (m, C1″/C2″), 144.2 (C4), 143.5 (m, C1″/C2″), 142.0 (m, C1), 139.9 (d, $^{2}J_{CP}$ = 11 Hz, C2), 137.7 (C3′), 137.3 (m, C6″), 133.4 (d, $^{2}J_{CP}$ = 9.6 Hz, C3″), 133.2 (d, $^{2}J_{CP}$ = 9.1 Hz, C3″), 132.1 (d, $^{1}J_{CP}$ = 10.2 Hz, C4″/C5″), 131.1 (d, $^{2}J_{CP}$ = 14.2 Hz, C4″/C5″), 126.6 (d, $^{2}J_{CP}$ = 20 Hz, C6), 123.3 (d, $^{3}J_{CP}$ = 7 Hz, C5), 122.8 (C4′), 119.7 (C2′), 96.4 (d, $^{1}J_{RhC}$ = 6 Hz, Cp*), 28.2 (m, C1‴),

24.3 (m, C1‴), 20.3 (m, C2‴), 19.4 (C2‴), 17.9 (d, $^{2}J_{CP}$ = 5 Hz, C2‴), 9.3 (Cp*–Me) ppm. $^{31}P\{^{1}H\}$ NMR (161.97 MHz, CD_2Cl_2): δ = 63.4 (dd, $^{2}J_{PP}$ = 98.6, 15.2 Hz, 2 P, $P_{terminal}$), 5.9 (t, $^{2}J_{PP}$ = 98.7 Hz, 1 P, $P_{central}$) ppm.

HR-MS (CH_3OH): ($C_{45}H_{58}AuCl_2NP_3Rh$; $[M - Cl]^+$, pos. ESI) calcd: 1040.2186 found: 1040.2214.

FT-IR (KBr): $\tilde{\nu}$ (cm^{-1}) = 3046 (w), 2957 (s), 2923 (s), 2866 (m), 1719 (m), 1601 (s), 1560 (s), 1468 (s), 1422 (m), 1382 (m), 1314 (w), 1239 (m), 1160 (w), 1107 (m), 1025 (m), 881 (m), 775 (m), 721 (w), 661 (m), 630 (w), 583 (w), 526 (m), 453 (w), 434 (m).

10: ^{1}H NMR ($CDCl_3$): δ (ppm) = 8.67 (dt, $^{3}J_{HH}$ = 5.6 Hz, $^{4}J_{HH}$ = 1.1 Hz, 1 H, 5′-H), 8.13 (m, 1 H, 6″-H), 7.92 (m, 1 H, 6″-H), 7.74 (d, $^{3}J_{HH}$ = 8.2 Hz, 1 H, 2′-H), 7.69–7.59 (m, 3 H, 3′- and 3″-H), 7.59–7.41 (m, 4 H, 4″- and 5″-H), 7.49 (dd, $^{3}J_{HH}$ = 8.1, $^{3}J_{PH}$ = 2.4 Hz, 1 H, 5-H), 7.46 (dd, $^{3}J_{PH}$ = 6.8 Hz, $^{4}J_{HH}$ = 1.6 Hz, 1 H, 2-H), 7.07 (ddd, $^{3}J_{HH}$ = 7.3, 5.7 Hz, $^{4}J_{HH}$ = 1.4 Hz, 1 H, 4′-H), 6.68 (td, $^{3}J_{PH,HH}$ = 8.4 Hz, $^{4}J_{HH}$ = 1.7 Hz, 1 H, 6-H), 2.82–2.65 (m, 4 H, 1‴-H), 1.48 (s, 15 H, Cp*–Me), 1.47–1.37 (m, 12 H, 2‴-H), 1.28 (ddt, $^{3}J_{PH}$ = 10.4 Hz, $^{3}J_{HH}$ = 7.0, 3.4 Hz, 6 H, 2‴-H), 0.82 (dq, $^{3}J_{PH}$ = 14.0 Hz, $^{3}J_{HH}$ = 7.3 Hz, 6 H, 2‴-H). $^{13}C\{^{1}H\}$ NMR ($CDCl_3$) δ (ppm) = 166.6 (C1′), 163.4 (C3), 151.3 (C5′), 146.2 (m, C1″/C2″), 144.6 (m, C1″/C2″), 143.8 (m, C1), 138.6 (d, $^{2}J_{CP}$ = 10.6 Hz, C2), 137.0 (C3′), 136.9 (m, C6″), 132.2 (m, C3″), 132.0 (C4), 131.1 (m, C4″/C5″), 129.9 (C4″/C5″), 126.1 (d, $^{2}J_{PC}$ = 20.4 Hz, C6), 123.5 (d, $^{3}J_{CP}$ = 8.2 Hz, C5), 122.5 (C4′), 119.1 (C2′), 88.6 (C, Cp*), 27.4 (m, C1‴), 23.8 (m, C1‴), 20.4 (m, C2‴), 20.0 (m, C2‴), 19.2 (m, C2‴), 17.5 (C2‴), 17.4 (C2‴), 8.9 (Cp*–Me). $^{31}P\{^{1}H\}$ NMR (161.97 MHz, CD_2Cl_2): δ = 63.4 (dd, $^{2}J_{PP}$ = 98.6, 15.2 Hz, 2 P, $P_{terminal}$), 5.9 (t, $^{2}J_{PP}$ = 98.7 Hz, 1 P, $P_{central}$) ppm.

HR-MS (CH_3OH): ($C_{45}H_{58}AuCl_2IrNP_3$; pos. ESI) calcd for $[M - 2Cl + CN]^+$: 1121.3105, found: 1121.3150; calcd for $[M - Cl]^+$: 1130.2754, found: 1130.2795.

FT-IR (KBr): $\tilde{\nu}$ (cm^{-1}) = 3046 (w), 2957 (s), 2923 (s), 2866 (m), 1719 (m), 1601 (s), 1560 (s), 1468 (s), 1422 (m), 1383 (m), 1314 (w), 1239 (m), 1159 (w), 1107 (m), 1025 (m), 881 (w), 775 (m), 721 (w), 662 (m), 630 (w), 583 (w), 526 (m), 454 (w), 434 (m).

Anion exchange reaction: preparation of 11

$AgNTf_2$ (77.5 mg, 0.2 mmol, 2 equiv.) was added to an orange solution of the gold–iridium–triphosphane complex **10** (116.4 mg, 0.1 mmol, 1 equiv.) in ACN (10 ml) resulting in a colour change to yellow and the formation of a white precipitate (AgCl). After 15 min of stirring in the dark, the solution was filtered over Celite and the filtrate was checked by ^{31}P NMR spectroscopy. Due to instability upon removal of solvent or crystallisation, the complex was subjected to *in situ* characterisation and no yield was determined.

^{1}H NMR (CD_3CN): δ (ppm) = 8.70 (ddd, $^{3}J_{HH}$ = 5.8, $^{4}J_{HH}$ = 1.5, $^{5}J_{HH}$ = 0.8 Hz, 1 H, 5′-H), 8.30 (bs, 2 H, 6″-H), 7.99 (ddd, $^{3}J_{HH}$ = 8.3, $^{4}J_{HH}$ = 1.7, $^{5}J_{HH}$ = 0.8 Hz, 1 H, 2′-H), 7.97–7.91 (m, 1 H, 3′-H), 7.87 (m, 2 H, H3″-H), 7.82–7.73 (m, 4 H, 4″- and 5″-H), 7.71 (dd, $^{3}J_{HH}$ = 8.1, $^{4}J_{HH}$ = 2.3 Hz, 1 H, 5-H), 7.36 (ddd, $^{3}J_{HH}$ = 7.3, 5.7, $^{4}J_{HH}$ = 1.6 Hz, 1 H, 4′-H), 7.26 (dd, $^{3}J_{HP}$ = 7.0, $^{4}J_{HH}$ = 1.7 Hz, 1 H, 2-H), 6.79 (td, $^{3}J_{HH/HP}$ = 8.2, 1.7 Hz, 1 H, 6-H), 3.12 (m, 2 H, 1‴-H), 2.72 (m, 2 H, 1‴-H), 1.49 (s, 15 H, Cp*–Me), 1.48–1.40 (m, 6 H, 2‴-H), 1.32–1.19 (m, 12 H, 2‴-H), 0.87 (*pseudo*-ddd, *N* = 19.0, 12.2, 6.6 Hz, 6 H, 2‴-H). $^{13}C\{^{1}H\}$ NMR (CD_2Cl_2): δ (ppm) = 166.0 (C1′), 157.0 (C3), 152.5 (C5′), 145.4 (C4), 143.3 (d, $^{1}J_{CP}$ = 21.6 Hz, C1), 143.2 (m, C1″/C2″), 139.5 (C3′), 137.6 (C6″), 137.5 (m, C2), 134.3 (d, $^{2}J_{CP}$ = 9.6 Hz, C3″), 134.2 (1C, C4″/C5″), 133.1 (1C, C4″/C5″), 132.7 (m, 2C, C4″/C5″), 126.5 (d, $^{2}J_{CP}$ = 18.1 Hz, C6), 124.3 (C4′), 124.2 (d, $^{3}J_{CP}$ = 6.7 Hz, C5), 121.5 (C2′), 120.1 (C), 92.2 (C, Cp*), 26.8 (*pseudo*-td, *N* = 18.2, 10.0 Hz, C1‴), 22.6 (m, C1‴), 19.6 (bs, C2′′), 19.1 (m, C2‴), 19.0 (bs, C2‴), 18.6 (bs, C2‴), 17.0 (bs, C2‴), 8.0 (Cp*–Me). $^{31}P\{^{1}H\}$ NMR (CD_3CN) δ (ppm) = 71.9 (d, J_{PP} = 70.0 Hz, 1 P, $P_{terminal}$), 71.5 (d, J_{PP} = 70.5 Hz, 1 P, $P_{terminal}$), 17.0 (*pseudo*-t, J_{PP} = 70.3 Hz, 1 P, $P_{central}$).

Testing of catalytic activity

Allenyl ether rearrangement. In a young NMR tube flushed with argon, allene (0.025 mmol, 4.0 μL) was dissolved in 0.5 mL CD_2Cl_2 together with 1 equiv. 1,4-dinitrobenzene (0.025 mmol, 4.2 mg). After cooling the solution to 0 °C, the corresponding catalyst (complex **7** or **11**) was added in a concentration of 0.5 mol%. The reaction mixture was kept at 0 °C for 1 h, and the progress of the reaction was monitored by ^{1}H NMR spectroscopy.

Cycloisomerisation of *N*-propargyl benzamide. In a young NMR tube, *N*-propargyl benzamide (0.056 mmol, 9.0 mg) was dissolved in 0.6 mL CD_2Cl_2 together with 0.5 equiv. 1,4-dioxane (0.028 mmol, 2.4 μL). Then, 0.1 mol% of the corresponding catalyst (complex **7** or **11**) was added, and the reaction progress at room temperature was followed by ^{1}H NMR spectroscopy. If the cycloisomerisation was successful, a subsequent reaction was performed in the same NMR tube by adding 2 equiv. $HSiEt_3$ and an additional catalyst loading of 0.9 mol%.

Data availability

The data supporting this article have been included as part of the ESI.†

Conflicts of interest

There are no conflicts to declare.

Acknowledgements

We appreciate the financial support from the German Israeli Foundation for Scientific Research and Development (GIF) and the Graduate School Building with Molecules and Nano-objects (BuildMoNa). We thank Manuela Roßberg for the elemental analysis, Ramona Oehme for the measurement of the mass spectra.

References

1 P. G. Gildner and T. J. Colacot, *Organometallics*, 2015, **34**, 5497.
2 H. Steinhagen and G. Helmchen, *Angew. Chem., Int. Ed. Engl.*, 1996, **35**, 2339.
3 J. A. Tainer, E. D. Getzoff, J. S. Richardson and D. C. Richardson, *Nature*, 1983, **306**, 284.
4 J.-H. Jeoung and H. Dobbek, *Science*, 2007, **318**, 1461.
5 M. Can, F. A. Armstrong and S. W. Ragsdale, *Chem. Rev.*, 2014, **114**, 4149.
6 J. H. H. Ho, J. Wagler, A. C. Willis and B. A. Messerle, *Dalton Trans.*, 2011, **40**, 11031.
7 B. G. Cooper, J. W. Napoline and C. M. Thomas, *Catal. Rev. - Sci. Eng.*, 2012, **54**, 1.
8 P. Buchwalter, J. Rosé and P. Braunstein, *Chem. Rev.*, 2015, **115**, 28.
9 J.-C. Wasilke, S. J. Obrey, R. T. Baker and G. C. Bazan, *Chem. Rev.*, 2005, **105**, 1001.
10 J. A. Mata, F. E. Hahn and E. Peris, *Chem. Sci.*, 2014, **5**, 1723.
11 R. G. Pearson, *J. Am. Chem. Soc.*, 1963, **85**, 3533.
12 M. Albrecht and G. van Koten, *Angew. Chem., Int. Ed.*, 2001, **40**, 3750.
13 G. Bauer and X. Hu, *Inorg. Chem. Front.*, 2016, **3**, 741.
14 M. A. W. Lawrence, K.-A. Green, P. N. Nelson and S. C. Lorraine, *Polyhedron*, 2018, **143**, 11.
15 M. S. Balakrishna, *Polyhedron*, 2018, **143**, 2.
16 L. Maser, L. Vondung and R. Langer, *Polyhedron*, 2018, **143**, 28.
17 E. Peris and R. H. Crabtree, *Chem. Soc. Rev.*, 2018, **47**, 1959.
18 C. M. Jensen, *Chem. Commun.*, 1999, 2443–2449.
19 D. Benito-Garagorri and K. Kirchner, *Acc. Chem. Res.*, 2008, **41**, 201.
20 Z. B. G. Fickenscher, P. Lönnecke, A. K. Müller, O. Hollóczki, B. Kirchner and E. Hey-Hawkins, *Molecules*, 2023, **28**, 2574.
21 Z. B. G. Fickenscher, L. Torres-Texeira, P. Lönnecke and E. Hey-Hawkins, *Inorg. Chim. Acta*, 2023, **558**, 121721.
22 Z. B. G. Fickenscher, P. Lönnecke, A. K. Müller, W. Baumann, B. Kirchner and E. Hey-Hawkins, *Inorg. Chem.*, 2023, **62**, 12750.
23 L. Li, W. W. Brennessel and W. D. Jones, *Organometallics*, 2009, **28**, 3492.
24 W. Voskuil and J. F. Arens, *Org. Synth.*, 1973, **5**, 211.
25 Rigaku Corporation, *CrysAlisPro Software System*, Rigaku Oxford Diffraction, Wroclaw, Poland, 1995–2023.
26 R. C. Clark and J. S. Reid, *Acta Crystallogr., Sect. A: Found. Crystallogr.*, 1995, **51**, 887.
27 G. M. Sheldrick, *Acta Crystallogr., Sect. A: Found. Adv.*, 2015, **71**, 3.
28 G. M. Sheldrick, *Acta Crystallogr., Sect. C: Struct. Chem.*, 2015, **71**, 3.
29 K. Brandenburg, *DIAMOND 4, version 4.6.8*, Crystal Impact GbR, Bonn, Germany.
30 L. Li, W. W. Brennessel and W. D. Jones, *J. Am. Chem. Soc.*, 2008, **130**, 12414.
31 M. Brasse, J. Cámpora, J. A. Ellman and R. G. Bergman, *J. Am. Chem. Soc.*, 2013, **135**, 6427.
32 A. I. VanderWeide, W. W. Brennessel and W. D. Jones, *J. Org. Chem.*, 2019, **84**, 12960.
33 D. L. Davies, K. Singh and N. Tamosiunaite, *Dalton Trans.*, 2021, **50**, 13505.
34 R. Romeo, L. A. Wozniak and C. Chatgilialoglu, *Tetrahedron Lett.*, 2000, **41**, 9899.
35 D. V. Griffiths, H. J. Groombridge, P. M. Mahoney, S. P. Swetnam, G. Walton and D. C. York, *Tetrahedron*, 2005, **61**, 4595.
36 M. Hayashi, *Chem. Lett.*, 2021, **50**, 1.
37 Y. Hu, L. Li, A. P. Shaw, J. R. Norton, W. Sattler and Y. Rong, *Organometallics*, 2012, **31**, 5058.
38 S. P. C. Dunstan, P. C. Healy, A. N. Sobolev, E. R. T. Tiekink, A. H. White and M. L. Williams, *J. Mol. Struct.*, 2014, **1072**, 253.
39 J. A. Muir, M. M. Muir, L. B. Pulgar, P. G. Jones and G. M. Sheldrick, *Acta Crystallogr., Sect. C: Cryst. Struct. Commun.*, 1985, **41**, 1174.
40 K. Angermaier, E. Zeller and H. Schmidbaur, *J. Organomet. Chem.*, 1994, **472**, 371.
41 J. A. Muir, S. I. Cuadrado and M. M. Muir, *Acta Crystallogr., Sect. C: Cryst. Struct. Commun.*, 1991, **47**, 1072.
42 M. Böhmer, F. Kampert, T. T. Y. Tan, G. Guisado-Barrios, E. Peris and F. E. Hahn, *Organometallics*, 2018, **37**, 4092.
43 J. Schießl, J. Schulmeister, A. Doppiu, E. Wörner, M. Rudolph, R. Karch and A. S. K. Hashmi, *Adv. Synth. Catal.*, 2018, **360**, 2493.
44 D. Wang, R. Cai, S. Sharma, J. Jirak, S. K. Thummanapelli, N. G. Akhmedov, H. Zhang, X. Liu, J. L. Petersen and X. Shi, *J. Am. Chem. Soc.*, 2012, **134**, 9012.
45 C. N. Kona and C. V. Ramana, *Chem. Commun.*, 2014, **50**, 2152.
46 C. N. Kona, M. N. Patil and C. V. Ramana, *Org. Chem. Front.*, 2016, **3**, 453.
47 A. S. K. Hashmi, J. P. Weyrauch, W. Frey and J. W. Bats, *Org. Lett.*, 2004, **6**, 4391.
48 O. A. Egorova, H. Seo, Y. Kim, D. Moon, Y. M. Rhee and K. H. Ahn, *Angew. Chem., Int. Ed.*, 2011, **50**, 11446.
49 Y. Liu, P. Liu, B. Ling, G. Chen, T. Chen, Y. Li, S. Bi and D. Zhang, *Eur. J. Org. Chem.*, 2019, 6822.
50 J. Segato, W. Baratta, P. Belanzoni, L. Belpassi, A. Del Zotto and D. Zuccaccia, *Inorg. Chim. Acta*, 2021, **522**, 120372.